Check for updates

Proceedings of the ASME 2024 43rd International
Conference on Ocean, Offshore and Arctic Engineering
OMAE2024
June 9-14, 2024, Singapore, Singapore

OMAE2024-120821

Downloaded from http://asmedigitalcollection.asme.org/OMAE/proceedings-pdf/OMAE2024/87837/V05BT06A020/7361184/v05bt06a020-omae2024-120821.pdf by Newcastle University user on 05 November 2024

IDENTIFICATION OF HYDRODYNAMIC COEFFICIENTS IN NONLINEAR MANEUVERING MODEL FOR AN ESSO 190000 DWT TANKER BY LEAST-SQUARES SUPPORT VECTOR REGRESSION WITH LINEAR SYSTEM

Ming Han Chua[1,2], Ivan Tam[2,3], Arun Kr. Dev[2,3] Bin Liu[2,3,*]

[1]Engineering Cluster, Singapore Institute of Technology, Singapore
[2]Faculty of Science, Agriculture, and Engineering, Newcastle University, United Kingdom
[3]Newcastle Research & Innovation Institute (NewRIIS), Singapore

ABSTRACT

In this article, the least-squares support vector machine (LS-SVM) with linear system of equations is used to identify the hydrodynamic derivatives of a three degree-of-freedom (3-Dofs) maneuvering model for an ESSO 190000 dwt tanker. Instead of identifying the hydrodynamic derivative independently, the highly-correlated hydrodynamic derivatives are identified together by LS-SVM and subsequently distinguished in sets of linear system of equations. The issue of parameter drift is briefly discussed and diminished with the proposed approach. The training data are sampled from the simulated zigzag maneuver. The computational procedures and set up of the support vector machine are discussed in detail. A number of predicted maneuvers are compared with the reference maneuvers. Excellent accuracy and generality of the estimated maneuvering model are achieved based on the proposed system identification technique.

Keywords: system identification, ESSO tanker, least-squares support vector machine, hydrodynamic derivatives, parameter drift

1. INTRODUCTION

To analyze the hydrodynamic characteristics of a ship and design an autopilot, a mathematical maneuvering model should be developed to precisely describe the behavior characteristics of the ship. To integrate the maneuvering model with modern control systems, an accurate estimation of the ship maneuverability is critical to the success of the design. The accuracy of the estimation guarantees the effectiveness of prediction of the maneuvering model and allows detection of anomalous changes.

The system identification (SI)-based approach provides an effective and practical means to determine the hydrodynamic characteristics of a vessel, in which only the state information and inertia terms are required. The system identification incorporates a very wide research area with different techniques implemented for different mathematical models. Many SI techniques had been implemented on nonlinear mathematical model in the past, e.g, model reference method [1, 2], Extended Kalman Filter (EKF) [3–5], least squares [6, 7], maximum likelihood [8], recursive prediction error [9], frequency spectrum analysis [10], particle swarm optimization [11] and genetic algorithm [12].

Machine learning and the neural networks have been applied in a diverse scientific fields nowadays. More recently, the support vector machine, SVM, was firstly implemented by Luo and Zou (2009) [13] to identify the hydrodynamic derivatives of Abkowitz model from the free-running model test. Subsequently, SVM was successfully applied in many other cases [14–18]. In contrast to neural networks, SVM requires no initial estimation of parameters, possesses a good generalization performance and returns a global optimal and unique solution [19]. On the other hand, neural networks was also implemented by many authors [20, 21] to predict the maneuvers of a free-surface vessel with satisfactory accuracy.

The main issue in the system identification is to deal with the problem of parameter identifiability. It was reported by many authors [13–15, 22] that some hydrodynamic derivatives are highly-correlated and thus, impose a difficulty in the system identification process. This issue is proposed as parameter drift. In this article, a new approach is proposed to diminish the parameter drift by implementing the least-squares support vector machine together with linear system of equations, in which the highly-correlated hydrodynamic derivatives are identified together. Subsequently, the combined hydrodynamic derivatives are distinguished by forming sets of linear system of equations. The training data is collected from $10^\circ/10^\circ$ zigzag maneuver for an ESSO tanker. Excellent accuracy is achieved using the proposed system identification technique. The estimated hydrodynamic derivatives are used to predict the motions of ship in different maneuvers, e.g., $20^\circ/20^\circ$ zigzag and 35° turn circle maneuvers. The motion predicted by the estimated maneuvering model are compared with the results

*Corresponding author: bin.liu@newcastle.ac.uk

Copyright © 2024 by ASME

obtained from the reference maneuvering model.

The article is organized in the following structure. In Sect. 2.1, the nonlinear maneuvering model for an ESSO tanker is presented. Following that, the numerical formulation of the least-squares support vector machine is introduced in Sec. 2.2. The issue of parameter drift and the proposed approach to diminish the parameter drift are discussed in Sec. 2.3. Subsequently, the set up of the proposed system identification technique and predicted results are presented in Sec. 3. Finally, the concluding remarks are summarized in Sect. 4.

2. NUMERICAL FORMULATIONS

In this section, the numerical formulations of the nonlinear maneuvering model of an ESSO 190000 dwt tanker and least-squares support vector machine are introduced in detail. Subsequently, the origin of the parameter drift is briefly discussed. The highly-correlated hydrodynamic derivatives are identified together and distinguished in linear system of multiple designated maneuvers. The estimated hydrodynamic derivatives and maneuvers are presented in Sect. 3.

2.1 Nonlinear maneuvering model for an ESSO tanker

The popular ship maneuvering models include Abkowtiz (whole-ship) model [23], Mathematical Modular Group (MMG) model [24] and response model [25]. In this article, LS-SVM is used to identify a non-dimensional non-linear maneuvering model [26] for an ESSO 190000 dwt tanker presented in Equation (1). Two coordinate systems are used, the earth-fixed global inertial frame $o_0 - x_0 y_0 z_0$ and the body-fixed local moving frame $o_0 - x_0 y_0 z_0$. The z axis of the body-fixed local moving frame points downward and its origin is at the free surface level. The $x - y$ plane of two coordinate systems coincide. The initial locations of respective axes in both coordinate systems are parallel.

$$\dot{u} - vr = gX'' \tag{1a}$$
$$\dot{v} + ur = gY'' \tag{1b}$$
$$(Lk''_z)^2 \dot{r} + Lx''_G ur = gLN'' \tag{1c}$$

where the superscript of double prime denotes the non-dimensionalization in Bis system [27]. Bis system can be used for zero-speed as well as high-speed applications, because the division of speed U is avoided. g and $L = L_{pp}$ are the gravitational acceleration and the length of the ship, where L_{pp} is the length between perpendiculars. k''_z and x''_G defined in Equation (2) are the non-dimensional radius of gyration of the ship in yaw and non-dimensional x coordinate of the centre of gravity of the ship. I_z is the moment of inertia about z-axis. Here the ship is assumed geometrically symmetric, $y_G = 0.0$.

$$k''_z = L^{-1}\sqrt{I_z/m} \tag{2a}$$
$$x''_G = L^{-1} x_G \tag{2b}$$

X'', Y'' and N'' in Equation (3) are the generalized non-dimensionalized forces and moment in surge, the sway and yaw motions, respectively.

$$X'' = X''(\dot{u}, u, v, r, T, \zeta, c, \delta) \tag{3a}$$
$$Y'' = Y''(\dot{v}, u, v, r, T, \zeta, c, \delta) \tag{3b}$$
$$N'' = N''(\dot{r}, u, v, r, T, \zeta, c, \delta) \tag{3c}$$

where u, v and $r = \dot{\psi}$ respectively are the velocity in the surge (forward), the sway (starboard) and the yaw motion. ψ is the yaw angle (in the horizontal plane). T, ζ, c and δ are respectively the propeller thrust, the water depth parameter, the flow velocity at the rudder and the rudder angle. The overdot represent the time derivative of a variable. Therefore, the non-dimensional forces in surge, sway and yaw can be formulated as

$$\begin{aligned} gX'' = {} & X''_{\dot{u}}\dot{u} + L^{-1}X''_{uu}u^2 + X''_{vr}vr + L^{-1}X''_{vv}v^2 \\ & + L^{-1}X''_{c|c|\delta\delta}c|c|\delta^2 + L^{-1}X''_{c|c|\beta\delta}c|c|\beta\delta + X''_{\dot{u}\zeta}\dot{u}\zeta \\ & + L^{-1}X''_{uu\zeta}u^2\zeta + X''_{vr\zeta}vr\zeta \\ & + L^{-1}X''_{vv\zeta\zeta}v^2\zeta^2 + gT''(1-\hat{t}) \end{aligned} \tag{4a}$$

$$\begin{aligned} gY'' = {} & Y''_{\dot{v}}\dot{v} + L^{-1}Y''_{uv}uv + L^{-1}Y''_{v|v|}v|v| + L^{-1}Y''_{c|c|\delta}c|c|\delta \\ & + Y''_{ur}ur + L^{-1}Y''_{|c|c|\beta|\beta|\delta|}|c|c|\beta|\beta|\delta| + Y''_{ur\zeta}ur\zeta \\ & + L^{-1}Y''_{uv\zeta}uv\zeta + L^{-1}Y''_{|v|v\zeta}|v|v\zeta \\ & + L^{-1}Y''_{|c|c|\beta|\beta|\delta|\zeta}|c|c|\beta|\beta|\delta|\zeta + Y''_{\dot{v}\zeta}\dot{v}\zeta + Y''_T gT'' \end{aligned} \tag{4b}$$

$$\begin{aligned} gLN'' = {} & L^2(N''_{\dot{r}}\dot{r} + N''_{\dot{r}\zeta}\dot{r}\zeta) + N''_{uv}uv + LN''_{|v|r}|v|r \\ & + N''_{|c|c\delta}|c|c\delta + LN''_{ur}ur + N''_{|c|c|\beta|\beta|\delta|}|c|c|\beta|\beta|\delta| \\ & + LN''_{ur\zeta}ur\zeta + N''_{uv\zeta}uv\zeta + LN''_{|v|r\zeta}|v|r\zeta \\ & + N''_{|c|c|\beta|\beta|\delta|\zeta}|c|c|\beta|\beta|\delta|\zeta + LN''_T gT'' \end{aligned} \tag{4c}$$

$\hat{t}$ is the thrust deduction factor. The non-dimensionalized thrust T'' and flow velocity c at the rudder are defined as

$$gT'' = L^{-1}T''_{uu}u^2 + T''_{un}un + LT''_{|n|n}|n|n \tag{5a}$$
$$c^2 = c_{un}un + c_{nn}n^2 \tag{5b}$$

where c_{un} and c_{nn} are constant values. n is the rpm of the propeller shaft. The water depth parameter ζ is defined in Equation (6), where h and d are the water depth and draft of the ship respectively. It is used to incorporate the influence of water depth on the hydrodynamic derivatives, and β defines the drift angle.

$$\zeta = \frac{d}{h-d}; \quad \beta = v/u \tag{6}$$

The primary particulars of the ESSO 190000 dwt tanker is listed in Tab. 1.

2.2 Least-squares support vector machine

In this section, a brief overview of support vector machines [28] and least-squares support vector machines [29]. The support vector machine was originally derived in the statistical learning theory as early as 1960s and proposed for the applications of classification.

More recently, SVM was used in the applications of regression analysis, e.g., ε-Support Vector Machine (ε-SVM). Typically, the ε-SVM is solved as nonlinear regression problems

Downloaded from http://asmedigitalcollection.asme.org/OMAE/proceedings-pdf/OMAE2024/87837/V05BT06A020/7361184/v05bt06a020-omae2024-120821.pdf by Newcastle University user on 05 November 2024

Copyright © 2024 by ASME

Length between perpendiculars (L_{pp})	304.8 (m)
Beam (B)	47.17 (m)
Draft to design waterline (T)	18.46 (m)
Displacement (∇)	220000 (m^3)
L_{pp}/B	6.46
B/T	2.56
Block coefficient (C_B)	0.83
Design speed (u_0)	16 (knots)
Propeller Speed	80 (rpm)

TABLE 1: Primary particulars of an ESSO 190000 dwt tanker

by means of convex quadratic programs using Quadratic optimization. In LS-SVM, the inequality constraints is replaced by equality constraints and use a squared loss function instead of ε-insensitive loss function. In LS-SVR, the objective is to define an optimal hyperplane as shown in Equation (7)

$$
\begin{aligned}
f(\boldsymbol{x}_i) &= \boldsymbol{w}^T \cdot \varphi(\boldsymbol{x}_i) + b \qquad \forall i = 1, \ldots, N \\
&\quad (\boldsymbol{x}_i \in \mathbb{R}^n, \varphi(\boldsymbol{x}_i) \in \mathbb{R}^N, \boldsymbol{w} \in \mathbb{R}^n)
\end{aligned} \tag{7}
$$

where $f(\boldsymbol{x}_i)$ and b are the estimated scalar output with respect to $\boldsymbol{x}_i$ and the optimal bias of the system. $\mathbb{R}^n$ represents a Euclidean space of dimension n, e.g., $b \in \mathbb{R}^0$ indicates a scalar. $\boldsymbol{x}$ and $\boldsymbol{w}$ are the vector input of training set and the optimal weight matrix of system respectively. $\varphi(\boldsymbol{x})$ is a mapping function, which projects $\boldsymbol{x}$ into a high-dimensional feature space $\mathbb{R}^N (N \gg n)$.

Minimizing the empirical risk functional in the feature space with a squared loss term leads to the following primal optimization formulation in Equation (8).

$$
\text{min:} \quad f(\boldsymbol{w}, e) = \frac{1}{2}\boldsymbol{w}^T\boldsymbol{w} + \frac{1}{2}C\sum_{i=1}^{N} e_i^2 \tag{8a}
$$

$$
\text{s.t.:} \quad y_i = \boldsymbol{w}^T\varphi(\boldsymbol{x}_i) + b + e_i \quad i = 1, \ldots, N \tag{8b}
$$

where e_i is the error. C is the regularization parameter/structural risk, which balances the model accuracy and generality of the model. The optimization problem in Equation (8) can be formulated as a Lagrange function as shown below.

$$
\begin{aligned}
\mathscr{L}(\boldsymbol{w}, b, e_i, \alpha_i) &= \frac{1}{2}\boldsymbol{w}^T\boldsymbol{w} + \frac{1}{2}C\sum_{i=1}^{N} e_i^2 \\
&\quad - \sum_{i=1}^{N} \alpha_i \left[\boldsymbol{w}^T\varphi(\boldsymbol{x}_i) + b + e_i - y_i\right]
\end{aligned} \tag{9}
$$

where α_i is the Lagrange multiplier. In accordance to Karush-Kuhn-Tucker conditions (KKT) [29], Equation (9) can be solved and re-cast into the dual form as

$$
\frac{\partial \mathscr{L}}{\partial \boldsymbol{w}} = 0 \quad \longrightarrow \quad \boldsymbol{w} = \sum_{i=1}^{N} \alpha_i \varphi(\boldsymbol{x}_i) \tag{10a}
$$

$$
\frac{\partial \mathscr{L}}{\partial b} = 0 \quad \longrightarrow \quad \sum_{i=1}^{N} \alpha_i = 0 \tag{10b}
$$

$$
\frac{\partial \mathscr{L}}{\partial e_i} = 0 \quad \longrightarrow \quad \alpha_i = Ce_i \tag{10c}
$$

$$
\frac{\partial \mathscr{L}}{\partial \alpha_i} = 0 \quad \longrightarrow \quad \boldsymbol{w}^T\varphi(\boldsymbol{x}_i) + b + e_i - y_i = 0 \tag{10d}
$$

where $i = 1, \ldots, N$. N is the dimension of the feature space. By substituting Equation (10a) and Equation (10c) into Equation (10d), Equation (10b) and Equation (10d) can be re-cast into the state space form as shown below.

$$
\begin{bmatrix} 0.0 & \overrightarrow{\mathbf{1.0}}^T \\ \overrightarrow{\mathbf{1.0}} & \boldsymbol{K} + C^{-1}\boldsymbol{I} \end{bmatrix} \begin{bmatrix} b \\ \overrightarrow{\alpha} \end{bmatrix} = \begin{bmatrix} 0.0 \\ \overrightarrow{\boldsymbol{Y}} \end{bmatrix} \tag{11}
$$

where $\boldsymbol{I}$ is an identity matrix of $N \times N$, and $\overrightarrow{\mathbf{1.0}} = [1.0, \ldots, 1.0]^T$ is a unity vector. $\overrightarrow{\boldsymbol{Y}} = [y_1, \ldots, y_N]^T$ and $\overrightarrow{\alpha} = [\alpha_1, \ldots, \alpha_N]^T$. The kernel is defined as $K(\boldsymbol{x}_i \cdot \boldsymbol{x}_j) = \varphi(\boldsymbol{x}_i)^T\varphi(\boldsymbol{x}_j), i, j = 1, \ldots, N$, which is positive definite and satisfies the Mercer condition [30, 31]. In this work, the linear kernel function is used for system identification. Hence the optimal hyperplane can be formulated as

$$
y(\boldsymbol{x}_i) = \sum_{j=1}^{N} \alpha_i K(\boldsymbol{x}_i, \boldsymbol{x}_j) + b \quad i = 1, \ldots, N \tag{12}
$$

2.3 Parameter drift and linear system of hydrodynamic derivatives

The parameter drift is a severe issue in system identification of a free-surface vessel maneuvering models. Owing to the parameter drift, the values of highly-correlated hydrodynamic derivative trade off among each other. Hence, multiple sets of hydrodynamic derivatives can match with the solutions to the maneuvering model. It was reported that the mathematical origin of the parameter drift is (1) the dynamic cancellation for the linear terms [32, 33] and (2) the multicollinearity for the nonlinear terms [34]. Recently, it was reported that the parameter drift is also dependent upon different maneuvers [35], in which its physical significance was discussed.

Different approaches were proposed to diminish and alleviate the extent of parameter drift [34, 35]. In this article, a new approach is proposed to diminish the parameter drift by identifying the highly-correlated hydrodynamic derivatives together as a single parameter and subsequently distinguishing them via linear system of equations using multiple maneuvers. This approach is motivated by observation of the maneuvering model. For example, $X''_{uu\xi}$ is defined as the gradient of the force in the surge direction with respect to the variation of u and ξ. However, ξ is kept constant in each individual maneuver at a particular water depth. It means X''_{uu}, $X''_{uu\xi}$ and T''_{uu} are highly correlated during

Copyright © 2024 by ASME

Downloaded from http://asmedigitalcollection.asme.org/OMAE/proceedings-pdf/OMAE2024/87837/V05BT06A020/7361184/v05bt06a020-omae2024-120821.pdf by Newcastle University user on 05 November 2024

the maneuver, and the values of these three terms are going to trade off among themselves. The results from 10°/10° zigzag manoeuver at water depth 200 meter are taken as an example. The correlation coefficients of the hydrodynamic derivatives are listed in Table 2, 3 and 4. The highly correlated terms in surge, sway and yaw are highlighted with italic font, e.g., more than 95% correlated terms. It can be seen that the ξ, $\hat{t}$ and n are constant and redundant terms in the maneuver, and do not contribute to the gradients of the states. Hence u^2/L and $\xi u^2/L$ are highly correlated and so on.

To get rid of the influence of parameter drift, the highly correlated terms, e.g., X''_{uu}, $X''_{uu\xi}$ and T''_{uu} in surge, are identified together during system identification. The detailed procedures of identifying the hydrodynamic derivatives are presented below. To perform the system identification process, Equation (1) is re-cast into the following form.

$$(1 - X''_{\dot{u}} - X''_{\dot{u}\xi}\xi)\dot{u} = g''_1(u, v, r, T, \xi, c, \delta) \tag{13a}$$

$$(1 - Y''_{\dot{v}} - Y''_{\dot{v}\xi}\xi)\dot{v} = g''_2(u, v, r, T, \xi, c, \delta) \tag{13b}$$

$$(k_z^2 - N''_{\dot{r}} - N''_{\dot{r}\xi}\xi)\dot{r} = g''_3(u, v, r, T, \xi, c, \delta) \tag{13c}$$

The force terms g''_1, g''_2 and g''_3 are re-arranged as shown below.

$$g''_1 = \boldsymbol{w}_X^T \cdot \boldsymbol{A}_X \tag{14a}$$

$$g''_2 = \boldsymbol{w}_Y^T \cdot \boldsymbol{A}_Y \tag{14b}$$

$$g''_3 = \boldsymbol{w}_N^T \cdot \boldsymbol{A}_N \tag{14c}$$

where

$$\boldsymbol{w}_X = \begin{bmatrix} X''_{uu} + X''_{uu\xi}\xi + (1.0 - \hat{t})T''_{uu} \\ 1.0 + X''_{vr} + X''_{vr\xi}\xi \\ X''_{vv} + X''_{vv\xi\xi}\xi^2 \\ X''_{|c|c\delta\delta} \\ X''_{|c|c\beta\delta} \\ T''_{un} \\ T''_{|n|n} \end{bmatrix} \tag{15a}$$

$$\boldsymbol{w}_Y = \begin{bmatrix} Y''_{uv} + Y''_{uv\xi}\xi \\ Y''_{|v|v} + Y''_{|v|v\xi}\xi \\ Y''_{|c|c\delta} \\ Y''_{ur} - 1.0 + Y''_{ur\xi}\xi \\ Y''_{|c|c|\beta|\beta|\delta|} + Y''_{|c|c|\beta|\beta|\delta|\xi}\xi \\ Y''_T \end{bmatrix} \tag{15b}$$

$$\boldsymbol{w}_N = \begin{bmatrix} N''_{uv} + N''_{uv\xi}\xi \\ N''_{|v|r} + N''_{|v|r\xi}\xi \\ N''_{|c|c\delta} \\ N''_{ur} - x''_G + N''_{ur\xi}\xi \\ N''_{|c|c|\beta|\beta|\delta|} + N''_{|c|c|\beta|\beta|\delta|\xi}\xi \\ N''_T \end{bmatrix} \tag{15c}$$

$$\boldsymbol{A}_X = \begin{bmatrix} u^2/L \\ vr \\ v^2/L \\ |c|c\delta^2/L \\ |c|c\beta\delta/L \\ (1-\hat{t})un \\ (1-\hat{t})|n|nL \end{bmatrix} \tag{16a}$$

$$\boldsymbol{A}_Y = \begin{bmatrix} uv/L \\ |v|v/L \\ |c|c\delta/L \\ ur \\ |c|c|\beta|\beta|\delta|/L \\ gT \end{bmatrix} \tag{16b}$$

$$\boldsymbol{A}_N = \begin{bmatrix} uv/L^2 \\ |v|r/L \\ |c|c\delta/L^2 \\ ur/L \\ |c|c|\beta|\beta|\delta|/L^2 \\ gT/L \end{bmatrix} \tag{16c}$$

To illustrate the proposed computational procedures, the identification of hydrodynamic derivatives in surge is taken as an example and shown in Equation (17) to Equation (20). Here it is assumed the added-mass/acceleration terms, eg., $X''_{\dot{u}}$ and $X''_{\dot{u}\xi}$, and the performance of the thruster in open water, e.g., T''_{uu}, T''_{un}, $T''_{|n|n}$, c_{un}, c_{nn} and $\hat{t}$, are known a prior. For instance, two maneuvers at different water depth, $h = 200.0$ [m] and $h = 50.0$ [m], are simulated for the purpose of system identification. The solutions to the linear equations of the surge motion can be obtained as.

$$X''_{uu} + \frac{18.46}{200 - 18.46}X''_{uu\xi} + (1 - 0.22)\cdot(-0.00695) = -0.04359 \tag{17a}$$

$$X''_{uu} + \frac{18.46}{50 - 18.46}X''_{uu\xi} + (1 - 0.22)\cdot(-0.00695) = -0.04650 \tag{17b}$$

$$\Longrightarrow \begin{cases} X''_{uu} &= -0.0376 \\ X''_{uu\xi} &= -0.0060 \end{cases} \tag{17c}$$

$$1.0 + X''_{vr} + \frac{18.46}{200 - 18.46}X''_{vr\xi} = 2.05754 \tag{18a}$$

$$1.0 + X''_{vr} + \frac{18.46}{50 - 18.46}X''_{vr\xi} = 2.24333 \tag{18b}$$

$$\Longrightarrow \begin{cases} X''_{vr} &= 1.02 \\ X''_{vr\xi} &= 0.385 \end{cases} \tag{18c}$$

$$X''_{vv} + X''_{vv\xi\xi}\left(\frac{18.46}{200 - 18.46}\right)^2 = 0.29648 \tag{19a}$$

$$X''_{vv} + X''_{vv\xi\xi}\left(\frac{18.46}{50 - 18.46}\right)^2 = 0.29706 \tag{19b}$$

$$\Longrightarrow \begin{cases} X''_{vv} &= 0.300 \\ X''_{vv\xi\xi} &= 0.0017 \end{cases} \tag{19c}$$

Downloaded from http://asmedigitalcollection.asme.org/OMAE/proceedings-pdf/OMAE2024/87837/V05BT06A020/7361184/v05bt06a020-omae2024-120821.pdf by Newcastle University user on 05 November 2024

Copyright © 2024 by ASME

	u^2/L	$\xi u^2/L$	$(1-\hat{t})u^2/L$	vr	ξvr	v^2/L	$\xi^2 v^2/L$	$\|c\|c\delta^2/L$	$\|c\|c\beta\delta/L$	$(1-\hat{t})un$	$(1-\hat{t})\|n\|nL$
u^2/L	1.0	*1.0*	*1.0*	0.1054	0.1054	-0.2071	-0.2071	0.033	0.2234	*0.9994*	0.0
$\xi u^2/L$	–	1.0	*1.0*	0.1054	0.1054	-0.2071	-0.2071	0.033	0.2234	*0.9994*	0.0
$(1-\hat{t})u^2/L$	–	–	1.0	0.1054	0.1054	-0.2071	-0.2071	0.033	0.2234	*0.9994*	0.0
vr	–	–	–	1.0	*1.0*	*-0.9514*	*-0.9514*	0.3271	-0.3802	0.1023	0.0
ξvr	–	–	–	–	1.0	*-0.9514*	*-0.9514*	0.3271	-0.3802	0.1023	0.0
v^2/L	–	–	–	–	–	1.0	*1.0*	-0.3182	0.1018	-0.2097	0.0
$\xi^2 v^2/L$	–	–	–	–	–	–	1.0	-0.3182	0.1018	-0.2097	0.0
$\|c\|c\delta^2/L$	–	–	–	–	–	–	–	1.0	0.0314	0.0361	0.0
$\|c\|c\beta\delta/L$	–	–	–	–	–	–	–	–	1.0	0.2403	0.0
$(1-\hat{t})un$	–	–	–	–	–	–	–	–	–	1.0	0.0
$(1-\hat{t})\|n\|nL$	–	–	–	–	–	–	–	–	–	–	1.0

TABLE 2: Correlation coefficients of hydrodynamic derivatives in 10°/10° zigzag maneuver: surge and condition number = 3.7407 × 10^{16}

	uv/L	$uv\xi/L$	$\|v\|v/L$	$\|v\|v\xi/L$	$\|c\|c\delta/L$	ur	$ur\xi$	$\|c\|c\|\beta\|\beta\|\delta\|/L$	$\|c\|c\|\beta\|\beta\|\delta\|\xi/L$	gT
uv/L	1.0	*1.0*	*0.9663*	*0.9663*	0.1107	-0.9445	-0.9445	0.9472	0.9472	0.0026
$uv\xi/L$	–	1.0	*0.9663*	*0.9663*	0.1107	-0.9445	-0.9445	0.9472	0.9472	0.0026
$\|v\|v/L$	–	–	1.0	*1.0*	0.0992	-0.9164	-0.9164	*0.9748*	*0.9748*	0.0215
$\|v\|v\xi/L$	–	–	–	1.0	0.0992	-0.9164	-0.9164	*0.9748*	*0.9748*	0.0215
$\|c\|c\delta/L$	–	–	–	–	1.0	-0.4194	-0.4194	0.079	0.079	0.0036
ur	–	–	–	–	–	1.0	*1.0*	-0.8872	-0.8872	-0.0027
$ur\xi$	–	–	–	–	–	–	1.0	-0.8872	-0.8872	-0.0027
$\|c\|c\|\beta\|\beta\|\delta\|/L$	–	–	–	–	–	–	–	1.0	*1.0*	0.0223
$\|c\|c\|\beta\|\beta\|\delta\|\xi/L$	–	–	–	–	–	–	–	–	*1.0*	0.0223
gT	–	–	–	–	–	–	–	–	–	1.0

TABLE 3: Correlation coefficients of hydrodynamic derivatives in 10°/10° zigzag maneuver: sway and condition number = 8.544 × 10^{16}

Copyright © 2024 by ASME

Downloaded from http://asmedigitalcollection.asme.org/OMAE/proceedings-pdf/OMAE2024/87837/V05BT06A020/7361184/v05bt06a020-omae2024-120821.pdf by Newcastle University user on 05 November 2024

Downloaded from http://asmedigitalcollection.asme.org/OMAE/proceedings-pdf/OMAE2024/87837/V05BT06A020/7361184/v05bt06a020-omae2024-120821.pdf by Newcastle University user on 05 November 2024

$$X''_{|c|c\delta\delta} = -0.093 \tag{20a}$$

$$X''_{|c|c\beta\delta} = 0.152 \tag{20b}$$

The rest of estimated hydrodynamic derivatives are presented in the next section. Furthermore, the correlation coefficients of the hydrodynamic derivatives are analyzed again for the proposed system identification scheme in Table 5, 6 and 7 for surge, sway and yaw, respectively. It can be observed that the number of the highly correlated terms become very sparse via the proposed system identification scheme. In particular, the condition numbers of the covariance matrices are tremendously diminished by 13 orders of magnitudes, as shown in Table 2 to 7.

The set up of system identification and the results of the estimated hydrodynamic derivatives are presented in the next section. By identifying the hydrodynamic derivatives in this way, a more consistent method can be obtained.

3. RESULTS AND DISCUSSION

3.1 Set up for system identification

To obtain the training data, the simulated results from two $10^\circ/10^\circ$ zigzag maneuvers at different water depths, $h = 200.0$ [m] and $h = 50.0$ [m], and the same designed velocity $u_0 = 16.0$ [kn] are collected. The $20^\circ/20^\circ$ zigzag, 35° turn circle and $10^\circ/10^\circ$ zigzag maneuvers are taken as examples to compare the referential and predicted maneuvers subsequently. All simulations are conducted for the same time window, $t \in [0, 600]$ [sec]. The maneuvering results in the initial 200 [sec] are chosen for analysis, in order to investigate the transient characteristics of the states. The sampling time is $dt = 0.02$ [s]. To obtain excellent accuracy, the generality is compromised by tuning LS-SVR to its highest accuracy. Hence, the regularization parameter, C, is set at: $C = 1 \times 10^7$ for the surge and sway motions and $C = 1 \times 10^{11}$ for the yaw motion.

3.2 Determination of hydrodynamic derivatives

To identify each hydrodynamic derivative in Equation (4), two computational procedures are taken in the proposed system identification scheme in Sect. 2.3: (1) system identification using LS-SVM (2) solving linear system equations to distinguish highly correlated terms. In step (1), the highly correlated hydrodynamic derivatives are combined and identified together using LS-SVM, as shown in Equation (13) and (14). In order to distinguish the highly correlated terms, multiple maneuvers are taken at different problem setups in step (2). For instance, two maneuvers at different water depth $h = 200.0$ [m] and $h = 50.0$ [m] are chosen to form the linear system equations. It is important to ensure that the characteristic matrix of the formed linear system equation should be invertible, e.g., Equation (17) to Equation (19). This procedure can be generalized to the other maneuvering models, such that the redundant terms can be successfully separated in the linear system equations. Hence, a customized design of the combination of highly correlated hydrodynamic derivatives and the linear system equations should be derived for the system identification of a particular maneuvering model.

The referential and estimated hydrodynamic derivatives are listed in Table 8. It can be seen that the estimated results

	uv/L^2	$uv\xi/L^2$	$\lvert v\rvert r/L$	$\lvert v\rvert r\xi/L$	$\lvert c\rvert c\delta/L^2$	ur/L	$ur\xi/L$	$\lvert c\rvert c\lvert\beta\rvert\delta\rvert/L^2$	$\lvert c\rvert c\lvert\beta\rvert\delta\rvert\xi/L^2$	gT/L
uv/L^2	1.0	*1.0*	-0.9406	-0.9406	0.1107	-0.9445	-0.9445	0.9472	0.9472	0.0026
$uv\xi/L^2$	–	1.0	-0.9406	-0.9406	0.1107	-0.9445	-0.9445	0.9472	0.9472	0.0026
$\lvert v\rvert r/L$	–	–	1.0	*1.0*	-0.2822	*0.9517*	*0.9517*	-0.9414	-0.9414	-0.0192
$\lvert v\rvert r\xi/L$	–	–	–	1.0	-0.2822	*0.9517*	*0.9517*	-0.9414	-0.9414	-0.0192
$\lvert c\rvert c\delta/L^2$	–	–	–	–	1.0	-0.4194	-0.4194	0.079	0.079	0.0036
ur/L	–	–	–	–	–	1.0	*1.0*	-0.8872	-0.8872	-0.0027
$ur\xi/L$	–	–	–	–	–	–	1.0	-0.8872	-0.8872	-0.0027
$\lvert c\rvert c\lvert\beta\rvert\delta\rvert/L^2$	–	–	–	–	–	–	–	1.0	*1.0*	0.0223
$\lvert c\rvert c\lvert\beta\rvert\delta\rvert\xi/L^2$	–	–	–	–	–	–	–	–	1.0	0.0223
gT/L	–	–	–	–	–	–	–	–	–	1.0

TABLE 4: Correlation coefficients of hydrodynamic derivatives in $10^\circ/10^\circ$ zigzag maneuver: yaw and condition number = 7.7864×10^{16}

Copyright © 2024 by ASME

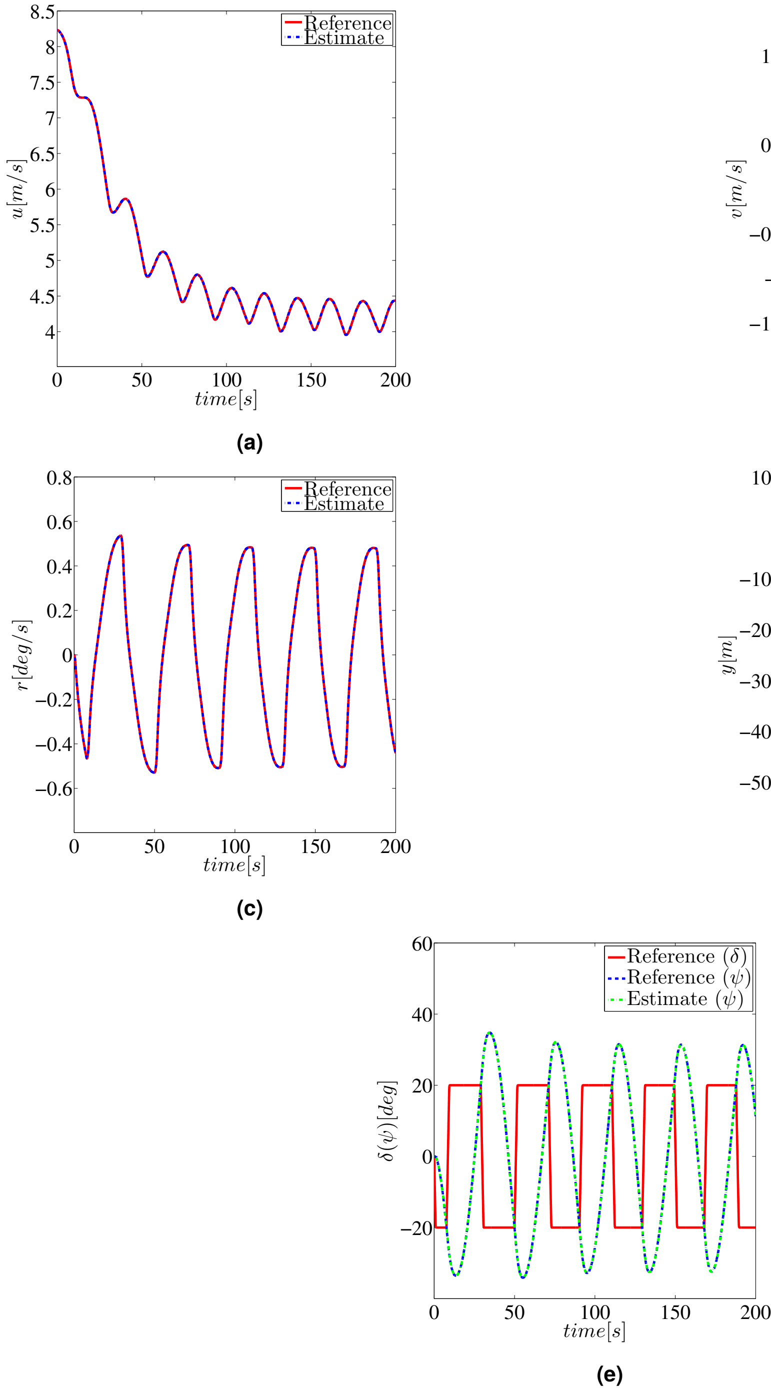

FIGURE 1: 20°/20° zigzag maneuver at h = 200.0 [m] and u_0 = 16.0 [kn] by LS-SVR and linear system: (a) u vs. time; (b) v vs. time; (c) r vs. time; (d) x vs. y; (e) ψ vs. time

Downloaded from http://asmedigitalcollection.asme.org/OMAE/proceedings-pdf/OMAE2024/87837/V05BT06A020/7361184/v05bt06a020-omae2024-120821.pdf by Newcastle University user on 05 November 2024

Copyright © 2024 by ASME

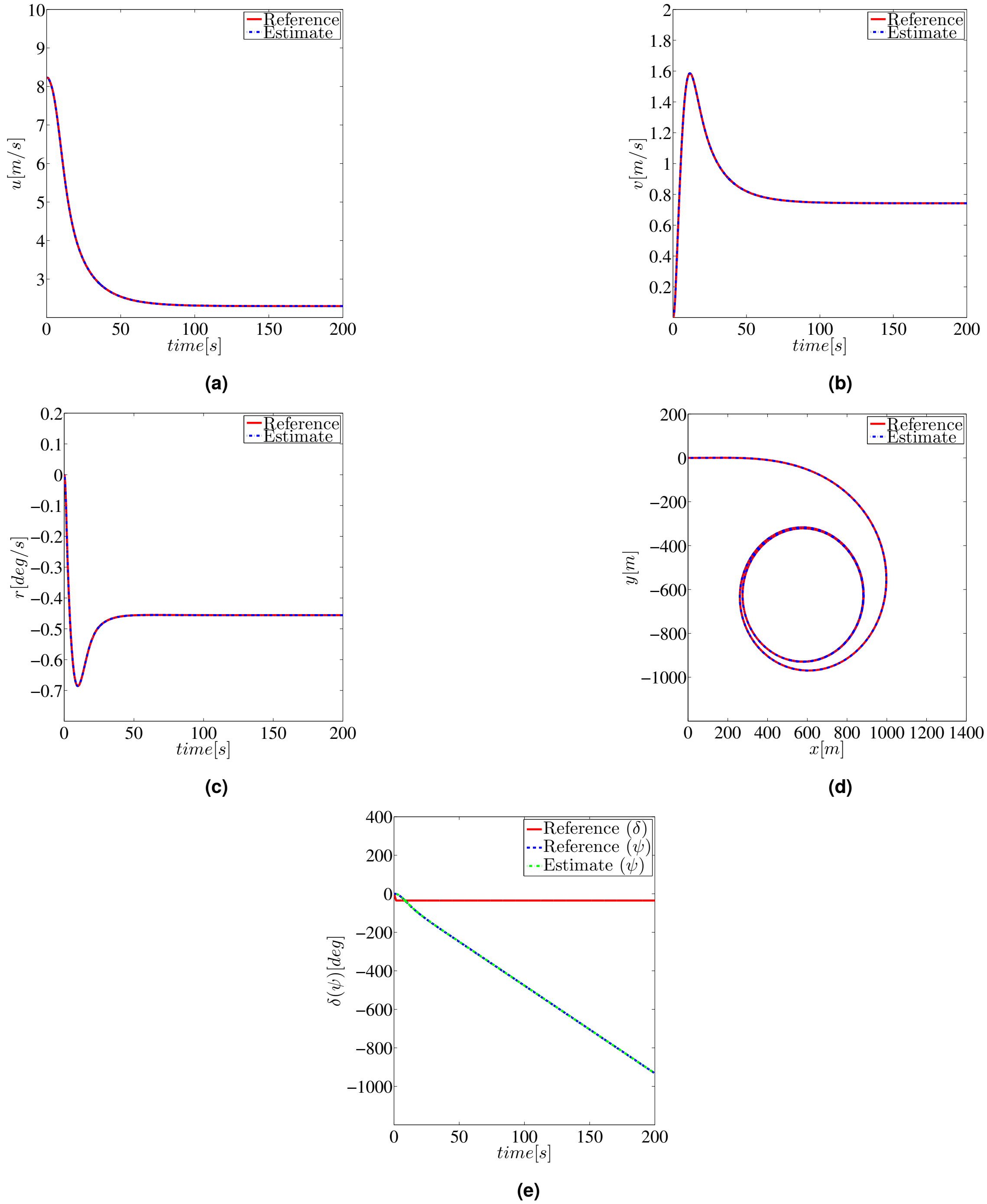

FIGURE 2: 35° turn circle maneuver at h = 200.0 [m] and u_0 = 16.0 [kn] by LS-SVR and linear system: (a) u vs. time; (b) v vs. time; (c) r vs. time; (d) x vs. y; (e) ψ vs. time

Downloaded from http://asmedigitalcollection.asme.org/OMAE/proceedings-pdf/OMAE2024/87837/V05BT06A020/7361184/v05bt06a020-omae2024-120821.pdf by Newcastle University user on 05 November 2024

Copyright © 2024 by ASME

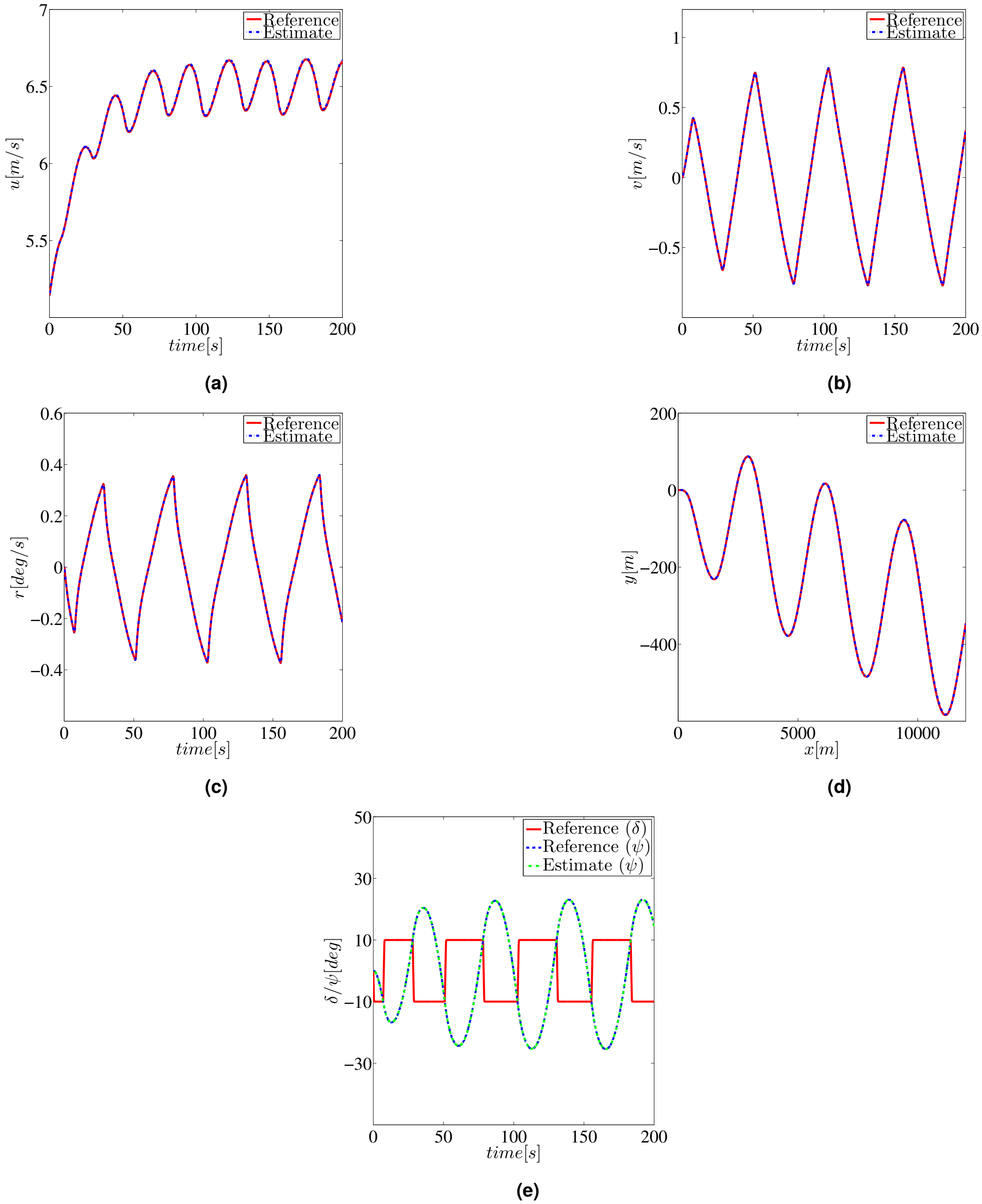

FIGURE 3: $10^\circ/10^\circ$ zigzag maneuver at h = 50.0 [m] and u_0 = 10.0 [kn] by LS-SVR and linear system: (a) u vs. time; (b) v vs. time; (c) r vs. time; (d) x vs. y; (e) ψ vs. time

Downloaded from http://asmedigitalcollection.asme.org/OMAE/proceedings-pdf/OMAE2024/87837/V05BT06A020/7361184/v05bt06a020-omae2024-120821.pdf by Newcastle University user on 05 November 2024

Copyright © 2024 by ASME

Downloaded from http://asmedigitalcollection.asme.org/OMAE/proceedings-pdf/OMAE2024/87837/V05BT06A020/7361184/v05bt06a020-omae2024-120821.pdf by Newcastle University user on 05 November 2024

	uv/L^2	$\|v\|r/L$	$\|c\|c\delta/L^2$	ur/L	$\|c\|c\|\beta\|\beta\|\delta\|/L^2$	gT/L
uv/L^2	1.0	-0.9406	0.1107	-0.9445	0.9472	0.0026
$\|v\|r/L$	–	1.0	-0.2822	*0.9517*	-0.9414	-0.0192
$\|c\|c\delta/L^2$	–	–	1.0	-0.4194	0.079	0.0036
ur/L	–	–	–	1.0	-0.8872	-0.0027
$\|c\|c\|\beta\|\beta\|\delta\|/L^2$	–	–	–	–	1.0	0.0223
gT/L	–	–	–	–	–	1.0

TABLE 7: Correlation coefficients of combined hydrodynamic derivatives in 10°/10° zigzag maneuver: yaw and condition number = 1.0663 × 10^3

	u^2/L	vr	v^2/L	$\|c\|c\delta^2/L$	$\|c\|c\beta\delta/L$	$(1-\hat{t})un$	$(1-\hat{t})\|n\|nL$
u^2/L	1.0	0.1054	-0.2071	0.033	0.2234	0.9994	0.0
vr	–	1.0	*-0.9514*	0.3271	-0.3802	0.1023	0.0
v^2/L	–	–	1.0	-0.3182	0.1018	-0.2097	0.0
$\|c\|c\delta^2/L$	–	–	–	1.0	0.0314	0.0361	0.0
$\|c\|c\beta\delta/L$	–	–	–	–	1.0	0.2403	0.0
$(1-\hat{t})un$	–	–	–	–	–	1.0	0.0
$(1-\hat{t})\|n\|nL$	–	–	–	–	–	–	1.0

TABLE 5: Correlation coefficients of combined hydrodynamic derivatives in 10°/10° zigzag maneuver: surge and condition number = 5.7427 × 10^3

	uv/L	$\|v\|v/L$	$\|c\|c\delta/L$	ur	$\|c\|c\|\beta\|\beta\|\delta\|/L$	gT
uv/L	1.0	*0.9663*	0.1107	- 0.9445	0.9472	0.0026
$\|v\|v/L$	–	1.0	0.0992	- 0.9164	*0.9748*	0.0215
$\|c\|c\delta/L$	–	–	1.0	- 0.4194	0079	0.0036
ur	–	–	–	1.0	-0.8872	-0.0027
$\|c\|c\|\beta\|\beta\|\delta\|/L$	–	–	–	–	1.0	0.0223
gT	–	–	–	–	–	1.0

TABLE 6: Correlation coefficients of combined hydrodynamic derivatives in 10°/10° zigzag maneuver: sway and condition number = 1.1108 × 10^3

Copyright © 2024 by ASME

Surge	Reference [26]	Present	Sway	Reference [26]	Present
$X''_{\dot{u}}$	-0.050	–	$Y''_{\dot{v}}$	-1.020	–
$X''_{\dot{u}\xi}$	-0.050	–	$Y''_{\dot{v}\xi}$	-0.387	–
X''_{uu}	-0.0377	-0.0376	Y''_{uv}	-1.205	-1.205
$X''_{uu\xi}$	-0.0061	-0.0060	$Y''_{uv\xi}$	0 or -0.85(1.0-$\frac{0.8}{\xi}$)	0
X''_{vr}	1.020	1.020	$Y''_{\lvert v\rvert v}$	-2.400	-2.401
$X''_{vr\xi}$	0.387	0.385	$Y''_{\lvert v\rvert v\xi}$	-1.500	-1.500
X''_{vv}	0.300	0.300	$Y''_{\lvert c\rvert c\delta}$	0.208	0.208
$X''_{vv\xi\xi}$	0.0125	0.017	Y''_{ur}	0.248	0.248
$X''_{\lvert c\rvert c\delta\delta}$	-0.093	-0.093	$Y''_{ur\xi}$	0.182	0.182
$X''_{\lvert c\rvert c\beta\delta}$	0.152	0.152	$Y''_{\lvert c\rvert c\lvert\beta\rvert\beta\lvert\delta\rvert}$	-2.16	-2.16
			$Y''_{\lvert c\rvert c\lvert\beta\rvert\beta\lvert\delta\rvert\xi}$	-0.191	-0.191
			Y''_{T}	0.04	0.04
Yaw	Reference [26]	Present	Thruster	Reference [26]	Present
$(k_z)^2 - N''_{\dot{r}}$	0.1232	–	T''_{uu}	-0.00695	–
$N''_{\dot{r}\xi}$	-0.0045	–	T''_{un}	-0.000630	–
N''_{uv}	-0.451	-0.451	$T''_{\lvert n\rvert n}$	0.0000354	–
$N''_{uv\xi}$	-0.241	-0.241	$\hat{t}$	0.22	–
$N''_{\lvert v\rvert r}$	-0.300	-0.300	c_{un}	0.605	–
$N''_{\lvert v\rvert r\xi}$	-0.120	-0.120	c_{nn}	38.2	–
$N''_{\lvert c\rvert c\delta}$	-0.098	-0.098			
$N''_{ur} - x_G$	-0.231	-0.231			
$N''_{ur\xi}$	-0.047	-0.047			
$N''_{\lvert c\rvert c\lvert\beta\rvert\beta\lvert\delta\rvert}$	0.688	0.688			
$N''_{\lvert c\rvert c\lvert\beta\rvert\beta\lvert\delta\rvert\xi}$	0.344	0.344			
N''_{T}	-0.02	-0.02			

TABLE 8: Estimated non-dimensionalized hydrodynamic derivatives (Bis system)

Copyright © 2024 by ASME

Downloaded from http://asmedigitalcollection.asme.org/OMAE/proceedings-pdf/OMAE2024/87837/V05BT06A020/7361184/v05bt06a020-omae2024-120821.pdf by Newcastle University user on 05 November 2024

match very well with the referential values from Fossen et al. (1994) [26]. In terms of the value of $Y''_{uv\xi}$, 0 for $\xi < 0.8$ and -0.85(1.0-0.8/ξ) for $\xi \geqslant 0.8$. Because the training data are collected from the maneuvers at $\xi < 0.8$, the estimated value of $Y''_{uv\xi}$ is zero in Table 8. Those estimated hydrodynamic derivatives show that the proposed system identification approach using LS-SVR and linear system of equations can estimate the hydrodynamic derivatives precisely with respect to the referential values.

3.3 Prediction of maneuvers

The estimated hydrodynamic derivatives are substituted into the ESSO tanker maneuvering model. Its results are compared with those obtained from the referential hdyrodynamic derivatives. Three maneuvers are simulated for the purpose of comparison: (1) 20°/20° zigzag maneuver at $h = 200.0$ [m] and $u_0 = 16.0$ [kn]; (2) 35° turn circle maneuver at $h = 200.0$ [m] and $u_0 = 16$ [kn]; (3) 10°/10° zigzag maneuver at $h = 50.0$ [m] and $u_0 = 10.0$ [kn]. The results are plotted in Fig. 1, Fig. 2 and Fig. 3 for the 20°/20° zigzag, 35° turn circle and 10°/10° maneuvers respectively. The comparison show that the predicted results obtained from the estimated hydrodynamic derivatives match excellently with those obtained from referential values. The discrepancy between the prediction and the reference results are not noticeable.

4. CONCLUSIONS

The least-squares support vector machine together with linear system equations was implemented to identify the hydrodynamic derivatives of a maneuvering model of an ESSO 190000 dwt tanker. The issue of parameter drift was tackled by identifying the highly-correlated hydrodynamic derivatives together and subsequently distinguishing them via linear system of equations. The two basic computational procedures were involved in the proposed system identification scheme: (1) combining the highly correlated hydrodynamic derivatives and identifying them using LS-SVM; (2) forming linear system equations to distinguish the highly correlated hydrodynamic derivatives. The estimated hydrodynamic derivatives matched very well with the referential values in literature. The estimated hydrodynamic derivatives were subsequently used to predict the maneuvers of the ship. The predicted results matched precisely with the referential results. The present method is proven to reliably solve even highly correlated maneuvering models. It can be generalized to the other maneuvering models by a correct combination of the highly correlated hydrodynamic terms and an appropriate design of the linear system equations. Therefore it is applicable to a variety of vessels with potential for strong parameter drift, where existing methods may not be sufficiently robust.

REFERENCES

[1] Hayes, Michael Ney. "Parametric identification of nonlinear stochastic systems applied to ocean vehicle dynamics." (1971).

[2] Van Amerongen, Job. "Adaptive steering of ships—A model reference approach." *Automatica* Vol. 20 No. 1 (1984): pp. 3–14.

[3] Abkowitz, Martin A. "Measurement of hydrodynamic characteristics from ship maneuvering trials by system identification." Technical report no. 1980.

[4] Shi, CJ, Zhao, D, Peng, J and Shen, C. "Identification of ship maneuvering model using extended Kalman Filters." *Marine Navigation and Safety of Sea Transportation* (2009): pp. 105–110.

[5] Perera, Lokukaluge P, Oliveira, P and Guedes Soares, C. "System identification of nonlinear vessel steering." *Journal of Offshore Mechanics and Arctic Engineering* Vol. 137 No. 3 (2015).

[6] Holzhüter, T. "Robust Identification Scheme in an Adaptive Track-Controller for Ships." *Adaptive Systems in Control and Signal Processing 1989*. Elsevier (1990): pp. 461–466.

[7] Muñoz-Mansilla, Rocío, Aranda, Joaquín, Díaz, José Manuel and De La Cruz, J. "Parametric model identification of high-speed craft dynamics." *Ocean Engineering* Vol. 36 No. 12-13 (2009): pp. 1025–1038.

[8] Astrom, KJ. "Maximum likelihood and prediction error methods." *IFAC Proceedings Volumes* Vol. 12 No. 8 (1979): pp. 551–574.

[9] Zhou, Wei-Wu and Blanke, Mogens. "Identification of a class of nonlinear state-space models using RPE techniques." *1986 25th IEEE Conference on Decision and Control*: pp. 1637–1642. 1986. IEEE.

[10] Bhattacharyya, Sriman K and Haddara, Mahmoud R. "Parametric identification for nonlinear ship maneuvering." *Journal of ship research* Vol. 50 No. 3 (2006): pp. 197–207.

[11] Xiong, Hejing, Chen, Mianyun, Lin, Yi, Chen, Yongbing and Song, Yexin. "Parameters identification for ship motion model based on particle swarm optimization." *Kybernetes* (2010).

[12] Sutulo, Serge and Soares, C Guedes. "An algorithm for offline identification of ship manoeuvring mathematical models from free-running tests." *Ocean Engineering* Vol. 79 (2014): pp. 10–25.

[13] Luo, WL and Zou, ZJ. "Parametric identification of ship maneuvering models by using support vector machines." *Journal of Ship Research* Vol. 53 No. 1 (2009): pp. 19–30.

[14] Zhang, Xin-guang and Zou, Zao-jian. "Identification of Abkowitz model for ship manoeuvring motion using ε-support vector regression." *Journal of hydrodynamics* Vol. 23 No. 3 (2011): pp. 353–360.

[15] Wang, Xue-gang, Zou, Zao-jian, Hou, Xian-rui and Xu, Feng. "System identification modelling of ship manoeuvring motion based on ε-support vector regression." *Journal of Hydrodynamics* Vol. 27 No. 4 (2015): pp. 502–512.

[16] Wang, Xue-gang, Zou, Zao-jian, Yu, Long and Cai, Wei. "System identification modeling of ship manoeuvring motion in 4 degrees of freedom based on support vector machines." *China Ocean Engineering* Vol. 29 No. 4 (2015): pp. 519–534.

[17] Zhu, Man, Hahn, Axel, Wen, Yuanqiao and Bolles, A. "Parameter identification of ship maneuvering models using recursive least square method based on support vector machines." *TransNav: International Journal on Marine Navigation and Safety of Sea Transportation* Vol. 11 (2017).

Downloaded from http://asmedigitalcollection.asme.org/OMAE/proceedings-pdf/OMAE2024/87837/V05BT06A020/7361184/v05bt06a020-omae2024-120821.pdf by Newcastle University user on 05 November 2024

Copyright © 2024 by ASME

[18] Xu, Haitong, Hassani, Vahid, Hinostroza, MA and Soares, C Guedes. "Real-Time Parameter Estimation of Nonlinear Vessel Steering Model Using Support Vector Machine." *ASME 2018 37th International Conference on Ocean, Offshore and Arctic Engineering*: pp. V11BT12A009–V11BT12A009. 2018. American Society of Mechanical Engineers.

[19] Luo, Weilin and Cai, Wenlong. "Modeling of ship manoeuvring motion using optimized support vector machines." *Fifth International Conference on Intelligent Control and Information Processing*: pp. 476–478. 2014. IEEE.

[20] Rajesh, G and Bhattacharyya, SK. "System identification for nonlinear maneuvering of large tankers using artificial neural network." *Applied Ocean Research* Vol. 30 No. 4 (2008): pp. 256–263.

[21] Luo, Weilin and Zhang, Zhicheng. "Modeling of ship maneuvering motion using neural networks." *Journal of Marine Science and Application* Vol. 15 No. 4 (2016): pp. 426–432.

[22] Luo, Weilin and Li, Xinyu. "Measures to diminish the parameter drift in the modeling of ship manoeuvring using system identification." *Applied Ocean Research* Vol. 67 (2017): pp. 9–20.

[23] Abkowitz, Martin A. "Lectures on ship hydrodynamics–Steering and manoeuvrability." Technical report no. 1964.

[24] Ogawa, Atsushi and Kasai, H. "On the mathematical model of manoeuvring motion of ships." *International Shipbuilding Progress* Vol. 25 No. 292 (1978): pp. 306–319.

[25] Nomoto, Kensaku, Taguchi, Kenshi, Honda, Keinosuke and Hirano, Susumu. "On the steering qualities of ships." *Journal of Zosen Kiokai* Vol. 1956 No. 99 (1956): pp. 75–82.

[26] Fossen, T. I. et al. *Guidance and control of ocean vehicles*. Vol. 199. Wiley New York (1994).

[27] Fossen, T. I. *Handbook of marine craft hydrodynamics and motion control*. John Wiley & Sons (2011).

[28] Vapnik, V. N. *Statistical learning theory*. Wiley, New York (1998).

[29] Suykens, J. A. K. et al. *Least squares support vector machines*. World Scientific (2002).

[30] Vapnik, V. *The nature of statistical learning theory*. Springer science & business media (2013).

[31] Suykens, J. A. K. and Vandewalle, J. "Least squares support vector machine classifiers." *Neural processing letters* Vol. 9 No. 3 (1999): pp. 293–300.

[32] Hwang, W. "Cancellation effect and parameter identifiability of ship steering dynamics." *International Shipbuilding Progress* Vol. 29 No. 332 (1982): pp. 90–102.

[33] Clarke, D., Gedling, P. and Hine, G. "The application of manoeuvring criteria in hull design using linear theory." *Transactions of the Royal Institution of Naval Architects, RINA*. (1982).

[34] Luo, W. and Li, X. "Measures to diminish the parameter drift in the modeling of ship manoeuvring using system identification." *Applied Ocean Research* Vol. 67 (2017): pp. 9–20.

[35] Liu, B. and Magee, A. R. "Analysis of parameter drift in system identification of ship manoeuvre model using neural networks and support vector regression." *Applied Ocean Research (under review)* .

Downloaded from http://asmedigitalcollection.asme.org/OMAE/proceedings-pdf/OMAE2024/87837/V05BT06A020/7361184/v05bt06a020-omae2024-120821.pdf by Newcastle University user on 05 November 2024

Copyright © 2024 by ASME